2018–2031 Nucleic Acids Research, 2011, Vol. 39, No. 6 Published online 13 November 2010
doi:10.1093/nar/gkq950

NLP is a novel transcription regulator involved in *VSG* expression site control in *Trypanosoma brucei*

Mani Shankar Narayanan[1,2], Manish Kushwaha[1,2], Klaus Ersfeld[3], Alexander Fullbrook[1], Tara M. Stanne[1] and Gloria Rudenko[1,*]

[1]Division of Cell and Molecular Biology, Sir Alexander Fleming Building, Imperial College London, South Kensington, London SW7 2AZ, [2]Department of Biochemistry, University of Oxford, Oxford OX1 3QU and [3]Department of Biological Sciences and Hull York Medical School, University of Hull, Cottingham Road, Hull HU6 7RX, UK

Received June 16, 2010; Revised and Accepted September 29, 2010

ABSTRACT

***Trypanosoma brucei* mono-allelically expresses one of approximately 1500 variant surface glycoprotein (VSG) genes while multiplying in the mammalian bloodstream. The active *VSG* is transcribed by RNA polymerase I in one of approximately 15 telomeric *VSG* expression sites (ESs). *T. brucei* is unusual in controlling gene expression predominantly post-transcriptionally, and how ESs are mono-allelically controlled remains a mystery. Here we identify a novel transcription regulator, which resembles a nucleoplasmin-like protein (NLP) with an AT-hook motif. NLP is key for ES control in bloodstream form *T. brucei*, as NLP knockdown results in 45- to 65-fold derepression of the silent *VSG221* ES. NLP is also involved in repression of transcription in the inactive *VSG* Basic Copy arrays, minichromosomes and procyclin loci. NLP is shown to be enriched on the 177- and 50-bp simple sequence repeats, the non-transcribed regions around rDNA and procyclin, and both active and silent ESs. Blocking NLP synthesis leads to downregulation of the active ES, indicating that NLP plays a role in regulating appropriate levels of transcription of ESs in both their active and silent state. Discovery of the unusual transcription regulator NLP provides new insight into the factors that are critical for ES control.**

INTRODUCTION

An intriguing puzzle in transcriptional control is how organisms control the expression of very large numbers of highly similar genes in a mono-allelic fashion. Examples include regulation of the mammalian olfactory receptor family, in which an individual neuron has more than 1200 olfactory receptor genes, of which only one is activated at a time (1). This mono-allelic expression has been proposed to involve the interaction of the active receptor gene promoter with an activating H-enhancer element, although whether this event regulates the 'counting' observed remains controversial (2,3). Parasitic protozoa like the malaria parasite *Plasmodium falciparum* also mono-allelically express only one out of approximately 50 *VAR* genes encoding the VAR proteins present on the surface of the parasitized erythrocyte (4). Activation of a *VAR* promoter alone is sufficient for silencing endogenous *VAR* transcription (5,6), while a role for the *VAR* introns in mutually exclusive *VAR* expression remains controversial (4,7).

Similarly, the African trypanosome *Trypanosoma brucei* contains more than 1500 variant surface glycoprotein (VSG) genes of which one is mono-allelically expressed (8–10). *T. brucei* is the causative agent of African trypanosomiasis in humans, which is endemic to sub-Saharan Africa and is transmitted by tsetse flies. Central to its success as an extracellular pathogen is a protective VSG coat which is antigenically varied during the course of an infection. Key for antigenic variation to work, is the ability of an individual trypanosome to ensure that only one *VSG* is expressed at a time from one of approximately 15 telomeric ESs (11,12). A stringent control operates on the active ES. Selection for simultaneous full activation of a second ES is not tolerated, and leads to trypanosomes which appear to be alternately switching between the two ESs (13). In insect form *T. brucei* all ESs are to a great extent transcriptionally downregulated, although not to the degree observed in silent ESs in bloodstream form *T. brucei* (14,15). It is still mysterious how the 'counting' machinery behind the mono-allelic transcription of *VSG* ESs in bloodstream form *T. brucei* is mediated.

Initially, it was not apparent that changes in chromatin structure played a significant role in ES regulation in bloodstream *T. brucei*. For example, experiments using exogenous T7 RNA polymerase as a probe showed a likely

*To whom correspondence should be addressed. Tel: +44 207 594 8137; Fax: +44 207 584 2056; Email: gloria.rudenko@imperial.ac.uk

© The Author(s) 2010. Published by Oxford University Press.
This is an Open Access article distributed under the terms of the Creative Commons Attribution Non-Commercial License (http://creativecommons.org/licenses/by-nc/2.5), which permits unrestricted non-commercial use, distribution, and reproduction in any medium, provided the original work is properly cited.

role for chromatin in silencing ESs in insect form, but not in bloodstream form *T. brucei* where the mono-allelic exclusion of ESs operates (16). This viewpoint has recently been revisited. Active ESs in bloodstream form *T. brucei* have recently been shown to be highly depleted of nucleosomes compared with silent ESs (17,18). In addition, a number of proteins involved in epigenetic regulation have recently been shown to be instrumental for controlling ESs in bloodstream form *T. brucei*. These include *T. brucei* ISWI (member of the SNF2 superfamily of chromatin remodeling proteins) (19), the telomere binding protein RAP1 (20) and the histone modification enzyme DOT1B (21).

Here, we identify a novel protein with nucleoplasmin-like features (nucleoplasmin-like protein—NLP) as playing a key role in regulation of ESs in bloodstream form *T. brucei*. Knockdown of NLP results in 45- to 65-fold derepression of the silent *VSG221* ES. NLP is also implicated in silencing other transcriptionally inactive areas of the genome in bloodstream form *T. brucei* including the silent *VSG* Basic Copy arrays, minichromosomes and procyclin loci. We also find that after blocking NLP synthesis fully processive transcription of the active ES is compromised. NLP therefore plays a role in regulating appropriate transcription of ESs in both their active and inactive states.

MATERIALS AND METHODS

Trypanosome strains and culturing

Bloodstream form *T. brucei brucei* 427 was used for all experiments. Cells were cultured at 37°C with 5% CO_2 in HMI-9 medium supplemented with 20% fetal bovine serum (22). The *T. brucei* T3-NLP1 and *T. brucei* T3-NLP2 clones are cell lines which have the MC^{177}NLP RNAi construct integrated into minichromosomes in bloodstream form *T. brucei* T3-SM (19). These cells have an active *VSGT3* expression site (ES), and *eGFP* in the silent *VSG221* ES (19). Maintaining these cells on blasticidin selection allows the propagation of a population of trypanosomes homogeneous for expression of VSGT3. The *T. brucei* 121-NLP1 and *T. brucei* 121-NLP2 clones are analogous cell lines, but express VSG121 instead of VSGT3.

The *T. brucei* MCEP reporter cell line has a construct containing *eGFP* (Clontech) behind an ES promoter that is inserted into a minichromosome. The *T. brucei* VBEP reporter cell line contains *eGFP* behind an ES promoter that is inserted into a *VSG* Basic Copy array. The *T. brucei* EP1eGFP cell line has a construct containing *eGFP* inserted behind an endogenous EP1 procyclin promoter. These reporter cell lines were created in a derivative of the *T. brucei* 'single marker' cell line (23) where the pHNES221Pur1.6 construct containing the puromycin resistance gene is inserted immediately behind the active VSG221 ES promoter. The MC^{177}NLP RNAi construct was inserted into these different reporter lines, and derepression of eGFP was monitored after the induction of *NLP* RNAi using tetracycline.

Epitope tagging of NLP with the haemagglutinin (HA) epitope was performed using *T. brucei* 221GPI(VO2+) which has an active VO2 ES containing a neomycin resistance gene, and *eGFP* and a puromycin resistance gene in the silent *VSG221* ES (24). This cell line was transfected with the pMOTagHA–NLP construct to produce *T. brucei* HA–NLP (25). Knocking out the second *NLP* allele was performed by transfecting with the pBSphleoNLPKO construct to produce *T. brucei* HA–NLPKO. As knocking out the second *NLP* allele did not lead to an observable effect on growth, this indicates that the HA epitope tagged copy of NLP is fully functional.

Sequence analysis

Trypanosoma brucei NLP (accession number Tb927.10.5450) protein domains were identified using MyHits (ISB-SIB) and PROSITE. *T. brucei* NLP was compared with *Saccharomyces cerevisiae* Swi2p/Snf2p (accession number NM_001183709.1), *Arabidopsis thaliana* HMG-I/Y (accession number Y10836.1), *Drosophila melanogaster* Nucleoplasmin (Nlp) (accession number NP_524557), ISWI (accession number NM_078995.1) and D1 (accession number NM_079562.2), *Dario rerio* Nucleoplasmin2 (accession number NM_001123007.2), *Xenopus laevis* Nucleoplasmin2 (accession number BC157168.1) and Nucleoplasmin3 (accession number NM_001016456.2), *Mus musculus* Nucleoplasmin1 (accession number BC090843.1), Nucleoplasmin3 (accession number NM_008723.1) and HMGI-C (accession number NM_010441.2), and *Homo sapiens* Nucleoplasmin3 (accession number NM_006993.2) and HMG-I/HMG-Y (accession number NM_145899.2) using ClustalW (26). *T. brucei* TDP1 (accession number Tb927.3.3490) had earlier been identified as binding the ES promoter by (27).

DNA constructs

The MC^{177}NLP RNAi construct has an 835-bp fragment (positions 1522–2356) of the NLP open reading frame, which was amplified using primers 5′- tttgctcgagCGATG CTTGTGTCCG and 5′- gacaggatccTTGAGGCGGTTA CTG and inserted between the opposing T7 promoters of the $p2T7^{Ti}$-177 construct (28). The MCEP reporter construct has the ES promoter from rDES1 (14) upstream of *eGFP* with flanking tubulin RNA processing signals (29) and a blasticidin resistance gene. This construct can be inserted into *T. brucei* minichromosomes using the 177-bp repeat containing sequence from the $p2T7^{Ti}$-177 construct (28). The VBEP reporter construct has the ES promoter upstream of *eGFP* as described above, targeted into the VSG118 Basic Copy array. The *VSG118* Basic Copy array targeting fragment was PCR amplified from *T. brucei* 427 genomic DNA using primers 5′-tatggatccCT TAAGTGAGCCAACACACCAG and 5′-ctggaattcCTG ACGAACCTCTAGTTACCG. The EP1 reporter construct has *eGFP* as described above targeted behind an endogenous EP1 procyclin promoter. The EP1 procyclin targeting fragment was PCR amplified from *T. brucei* genomic DNA using primers: 5′-TCAGTGGTTGTGTG GTAG and 5′-TACTTCTTGGTGTAATTGAAGT.

The pMOTagHA–NLP construct for HA-epitope tagging NLP was derived from the pMOTag4H vector (25). A 2163-bp fragment (positions 708–2871) of the NLP open reading frame was cloned using primers 5′-gttggtaccTCTCCTGAACACGGGACTTTCAC and 5′-caactcgagCAACTCcAG-CCTTAGCTTGTTC. The pBSphleoNLPKO vector allowed the genetic knockout of an *NLP* allele. A 492-bp fragment immediately upstream of the NLP open reading frame was amplified using primers 5′-tagtctagaGTGATTACATTCCCTACT TTC and 5′-agggatccTTATCCGCCTGGTACTTCCCT. Similarly a 645-bp downstream targeting fragment was amplified using primers: 5′-tagaagcttTGGGTGTTAGG AAACCTTCAA and 5′-tagctcgagTCACCAAGCAAAT CAATACGA. Construct integration into the genome allowed the replacement of NLP sequences with a phleomycin resistance cassette.

The His-tagged NLP fusion protein used for immunization of rabbits to produce a polyclonal anti-NLP antibody was made by amplifying a 597-bp fragment (positions 880–1476) of the NLP open reading frame using primers: 5′-catggatccGTCACCACCAGTCTCAACCAG and 5′-catctcgagGAGATCGCTGTAGTACACAGG and inserting this fragment into the pRSETA vector (Invitrogen) for expression in *Escherichia coli*.

Analysis of nucleic acids and protein

Protein lysates were made by washing cells, and dissolving the pellet in boiling hot SDS gel loading buffer at a concentration of 10^5 cells μl^{-1} (30). Protein lysates were incubated at 100°C for 10 min prior to loading on 10% SDS polyacrylamide gels. Gels were blotted on to Hybond-P membrane (Amersham) and probed with rabbit polyclonal antibodies raised against NLP, BiP (gift of Jay Bangs, University of Wisconsin, USA) or HA epitope tag (ab9110 AbCam). Polyclonal anti-NLP antibody was raised in rabbits immunised against His-tagged NLP fusion protein (positions 880–1476 of the NLP open reading frame). Recombinant fusion protein was expressed in BL21(DE3)pLysS cells [OneShot BL21(DE3)pLysS, Invitrogen] and then purified using denaturing conditions with the ProBond purification system (Invitrogen) according to manufacturer's instructions. Antisera were produced by Eurogentec (Belgium) using standard immunization protocols.

Subnuclear localisation of NLP was determined using immunofluorescence microscopy. Cells were washed, fixed with paraformaldehyde (end concentration 2%) and then allowed to settle on glass slides. Fixed cells were permeabilized with 0.1% NP-40, and then reacted with a rabbit polyclonal anti-HA antibody (ab9110, AbCam) and an anti-rabbit secondary antibody coupled to Alexa-488 (Molecular Probes). Microscopy was performed using a Zeiss Axioplan 2 microscope, and images were taken using a Roper Scientific (Trenton, NJ) Cool Snap HQ camera, and analysed with Metamorph 6.20 imaging software (Universal Imaging, Downington, PA).

Transcript levels were quantitated using quantitiative RT–PCR. RNA was isolated using RNeasy kits (Qiagen). RNA was DNase treated using Turbo DNA Free kit (Ambion) and cDNA synthesised using Omniscript Reverse Transcriptase (Qiagen) and random hexamer primers (Promega). Quantitative PCR (qPCR) was performed as described in ref. (18) on a Roche LightCycler480 Real-Time PCR system using primers optimized for producing a single amplicon of the correct size and listed in Supplementary Table S1 or ref. (18). Transcript levels at each time point were normalized to levels of actin transcript at that time point for experiments using the VSGT3 expressors, and γ-tubulin for experiments using the VSG121 expressors, and then plotted as fold increase with respect to the 0 h time point.

Chromatin immunoprecipitation

Chromatin immunoprecipitation (ChIP) was performed as described in (18) with minor modifications. Bloodstream form cells were fixed for 1 h in 1% formaldehyde at room temperature. Glycine was added to a final concentration of 125 mM to stop the reaction. Chromatin was sheared by sonication (BioRuptor, Diagenode) to produce DNA in the range of 200–500 bp, and the extract was clarified by centrifugation at 15 000*g* at 4°C. The solution was pre-cleared by incubation with protein A-Sepharose CL-4B beads (GE Healthcare) for 90 min at 4°C before incubation with the relevant antibody (or with 'no antibody' as negative control) for 16 h. Antibodies used include a mouse monoclonal antibody against the HA epitope (antibody ab1424, AbCam) and anti-histone H3 (ab1791, AbCam). Each experiment was performed in triplicate and further analysis of ChIP material was performed by quantitative PCR (qPCR). ChIP material was analysed by qPCR using primers optimized for producing a single amplicon of the correct size and are listed in (18) or in Supplementary Table S1. Final quantitation of HA-epitope tagged ChIP material in the *T. brucei* HA–NLP or wild-type cell lines was obtained after subtracting values derived from material immunoprecipitated with the corresponding 'no antibody' control experiments from both of these cell lines. ChIP material was slot blotted on to Hybond-XL membranes (GE Healthcare) and hybridized with radio-labelled probes as described previously (18).

Flow cytometry

RNAi against NLP was induced in *T. brucei* by the addition of 750 ng ml^{-1} tetracycline. Cells were centrifuged and washed at specified time points. Flow cytometry was carried out using a Becton-Dickinson FACSCalibur and CellQuest (BD) software. The amount of derepression was expressed as fold derepression, and calculated by dividing mean FL1-H values of RNAi-induced cultures at each time point by the mean FL1-H values of uninduced cultures.

RESULTS

NLP is a nucleoplasmin-like protein which is essential in bloodstream form *T. brucei*

We initially identified *T. brucei* NLP in DNA affinity chromatography experiments as binding the transcriptionally silent 177-bp simple sequence repeats, which comprise the

bulk of the *T. brucei* minichromosomes (accession number Tb927.10.5450) (V. Tilston and K.E., unpublished data). NLP shows little sequence similarity with proteins in non-Kinetoplastid protozoa, but contains a nucleoplasmin-like domain ($e = 2.3 \times 10^{-3}$) as well as a DNA binding AT-hook motif ($e = 9.8 \times 10^{-3}$) (MyHits; ISB-SIB) (Figure 1A). A characteristic glutamate-rich region ($e = 3.8 \times 10^{-9}$) extends approximately from residues 600–670, partially overlapping the nucleoplasmin-like domain (PROSITE). Additionally, two coiled-coil regions extend between residues 429–458 and 586–691 (SMART, EMBL).

Nucleoplasmin was first identified in *Xenopus* oocytes as a highly abundant nuclear protein and has since been found in other higher eukaryotes (31,32). We aligned NLP from *T. brucei* with previously characterized nucleoplasmins from a number of higher eukaryotes using ClustalW (Figure 1B). We were able to detect certain conserved or similar amino acids in the *T. brucei* NLP nucleoplasmin-like domain as predicted using Hidden Markov Models (Pfam). These residues include a leucine residue at position 557, glycine residues at positions 560, 562 and 569 and several glutamate residues in the downstream glutamate-rich region, which is typical of the nucleoplasmin domain (Figure 1B). This polyglutamate region is one of the features shared by all nucleoplasmins, and is also found in *T. brucei* NLP (Supplementary Figure S1A). AT-hook domains are small DNA-binding motifs containing a central glycine–arginine–proline (GRP) tri-peptide sequence (33,34). In *T. brucei* NLP, the AT-hook motif has in addition to the GRP core, typical lysine and arginine residues preceding the core as well as other polar residues immediately downstream of GRP, including a characteristic lysine residue in the fourth position downstream (Supplementary Figure S1B) (34).

Western blot analysis using an anti-NLP antibody identified a ~120 kDA protein in both bloodstream and procyclic form *T. brucei* (Figure 1C). This is slightly larger than the expected size for NLP (predicted to be 107 kDa) but the minor difference in size could be the consequence of post-translational modifications. NLP is expressed at equivalent levels in both life-cycle stages. NLP is an essential protein in bloodstream form *T. brucei*, as induction of

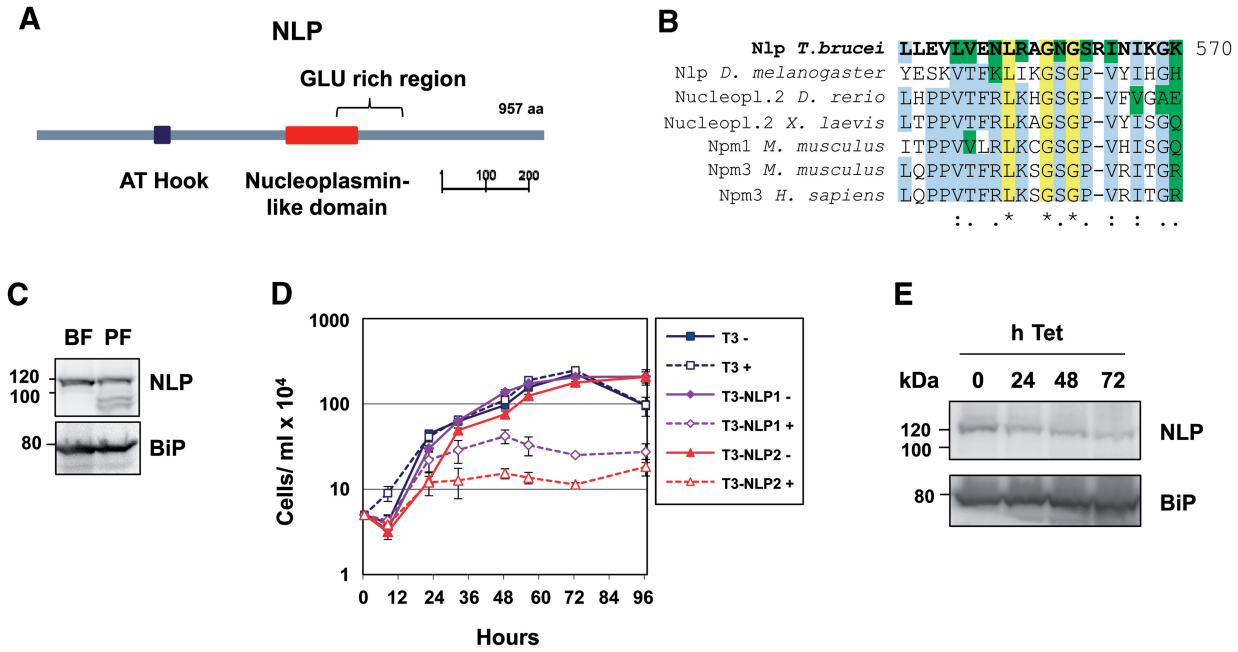

Figure 1. NLP is a nucleoplasmin-like DNA-binding protein. (**A**) Schematic of NLP with protein domains identified using PROSITE and MyHits (ISB-SIB). The NLP protein is 957 amino acids with an AT-hook domain extending from residues 214 to 226 represented with a dark blue rectangle, and a nucleoplasmin-like domain extending from residues 497 to 647 represented with a red rectangle. A glutamate (GLU)-rich region overlaps the nucleoplasmin-like domain and extends from residues 600 to 671. (**B**) Alignment using ClustalW of *T. brucei* NLP with nucleoplasmins from other eukaryotes. *T. brucei* NLP is compared with: *Drosophila melanogaster* Nucleoplasmin (Nlp), zebra fish (*Dario rerio*) Nucleoplasmin2, *Xenopus laevis* Nucleoplasmin2, *Mus musculus* Nucleoplasmin1 (Npm1) and Nucleoplasmin3 (Npm3) and *Homo sapiens* Nucleoplasmin3 (Npm3). Sequence accession numbers are listed in the 'Materials and Methods' section. A conserved region characteristic of nucleoplasmins is shown. Particularly conserved amino acids are indicated with yellow blocks and asterisks. Amino acids that are conserved in five to six sequences are highlighted with light blue blocks, and amino acids which are changed but have similar properties are indicated in green. Double dots indicate conservative and single dots indicate semi-conservative amino acid changes across all sequences as defined by ClustalW (26). (**C**) NLP is expressed at approximately equal levels in both bloodstream form (BF) and procyclic form (PF) *T. brucei*. Lysates from 1×10^7 cells were analysed on SDS–PAGE gels and the blots were probed with an antibody against NLP, or the loading control BiP. Size markers in kiloDaltons are indicated on the left. (**D**) Blocking synthesis of NLP by the induction of tetracycline inducible RNA interference in bloodstream form *T. brucei* T3-NLP1 and T3-NLP2 leads to growth arrest within 24 h. Cell lines that have been grown in the presence (+) or absence (−) of tetracycline are compared. The parental *T. brucei* T3 cell line is shown for comparison. (**E**) Reduction in NLP protein as confirmed by Western blot analysis using an anti-NLP antibody (NLP). Protein lysates were isolated from *T. brucei* T3NLP1 after the induction of NLP RNAi with tetracycline (Tet) for the time in hours (h) indicated above. The blot was also probed with an anti-BiP antibody as a loading control. Size markers in kiloDaltons are shown on the left.

NLP RNAi in the two *T. brucei* clones T3-NLP1 and T3-NLP2 leads to an abrupt growth arrest within 24 h of the addition of tetracycline (Figure 1D). Western blot analysis confirmed the knockdown of the NLP protein to 55% of normal levels by 48 h, and to <50% after 72 h induction of *NLP* RNAi (Figure 1E). Although a clear growth arrest was observed after the induction of *NLP* RNAi, this was not correlated with a significant accumulation of cells at any particular stage of the trypanosome cell cycle (results not shown).

We next made *T. brucei* cell lines which had an endogenous allele of NLP tagged with the HA epitope (Figure 2A). Cells with one *NLP* allele tagged with the HA-epitope grew as well as the parental *T. brucei* GPI(VO2+) cell line. Knocking out the second *NLP* allele in these lines, and thereby making the cells dependent on the one HA-tagged copy of NLP did not lead to an observable change in cell growth (result not shown). This indicates that addition of the HA-epitope to the carboxy terminus of NLP does not observably compromise NLP function. Microscopic analysis of *T. brucei* lines with a copy of HA-tagged NLP showed that NLP is a nuclear protein with a relatively even distribution through the nucleus throughout the cell cycle (Figure 2B).

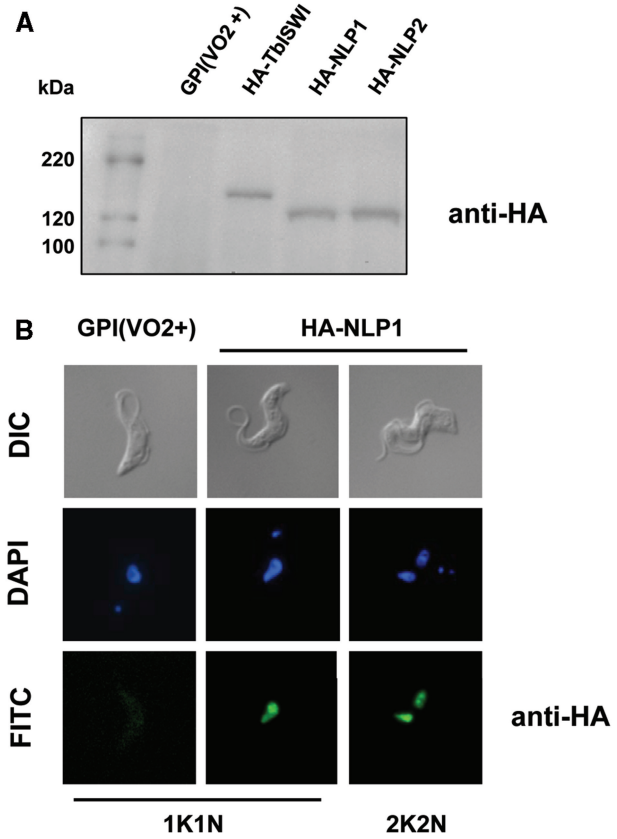

Figure 2. NLP is a nuclear protein. (**A**) Bloodstream form *T. brucei* cell lines expressing HA-epitope tagged NLP were generated (*T. brucei* HA–NLP1 and HA–NLP2). Protein lysates from these cell lines were compared with those from the parental *T. brucei* GPI(VO2+) cell line and *T. brucei* HA–TbISWI as a control for HA antibody specificity. (**B**) HA-epitope tagged NLP localizes to the nucleus. Panels show trypanosomes visualized using differential interference contrast (DIC), the DNA stain DAPI, or the FITC channel after immunofluorescence using a rabbit polyclonal anti-HA antibody and an anti-rabbit Alexa-488 secondary antibody. Cells containing either one kinetoplast (K) and one nucleus (N) (1K1N) or precytokinesis cells containing two kinetoplasts and two nuclei (2K2N) are shown.

Blocking synthesis of NLP results in derepression of silent ESs as well as other transcriptionally silent regions

As NLP had originally been identified as a DNA-binding protein binding the transcriptionally inactive *T. brucei* 177-bp repeats, we investigated if it plays a role in silencing inactive genomic regions. We first investigated its role in maintaining the repressed status of the silent *VSG* ESs. The bloodstream form *T. brucei* T3-SM cell line has a construct containing *eGFP* inserted immediately downstream of the promoter of the silent *VSG221* ES allowing monitoring for ES derepression with flow cytometry (19) (Figure 3A). In this cell line a blasticidin resistance gene has been inserted into the VSGT3 ES, allowing the maintenance of a population homogeneous for expression of VSGT3 in the presence of blasticidin selection. We induced RNAi against *NLP* using tetracycline, and followed ES derepression by flow cytometry.

Induction of *NLP* RNAi resulted in a striking 45- to 65-fold derepression of the silent *VSG221* ES after 72 h of induction of *NLP* RNAi (Figure 3B). In contrast, ES derepression was not observed when we induced RNAi against the essential DNA binding protein TDP1 (27) (Supplementary Figure S2), indicating that increased expression of *eGFP* was not simply a stress response caused by the absence of an essential protein or an artefact as a result of RNAi induced cell death. We also induced RNAi against *NLP* in the the *T. brucei* 121-SM cell line (19). This is an analogous bloodstream form *T. brucei* reporter cell line, with the *VSG121* ES active rather than the *VSGT3* ES. Here we observed 19- to 52-fold derepression of *eGFP* (Supplementary Figure S3).

Given the abundance of NLP in the nucleus, it seemed unlikely that its biological role was restricted to ES silencing. We were therefore next interested in determining the role of NLP in silencing other transcriptionally inactive areas of the *T. brucei* genome. In *T. brucei,* both rDNA promoters and ES promoters are transcribed by RNA polymerase I (35). Of the two promoters, transcription from the core ES promoter appears to be more sensitive to its chromosomal context. For example, an exogenous ES promoter was shown to be more comprehensively silenced than a comparable rDNA promoter when inserted in the transcriptionally silent *VSG* Basic Copy arrays (36). This observation allows the use of the ES promoter as a 'probe' for repressed chromatin regions (37).

As *T. brucei* NLP had originally been identified as a protein binding the 177-bp repeats, we investigated its role in silencing the *T. brucei* minichromosomes, which are comprised primarily of arrays of these simple sequence repeats (38). We therefore integrated a construct containing an ES core promoter upstream of *eGFP* into *T. brucei* minichromosomes (*T. brucei* MCEP in

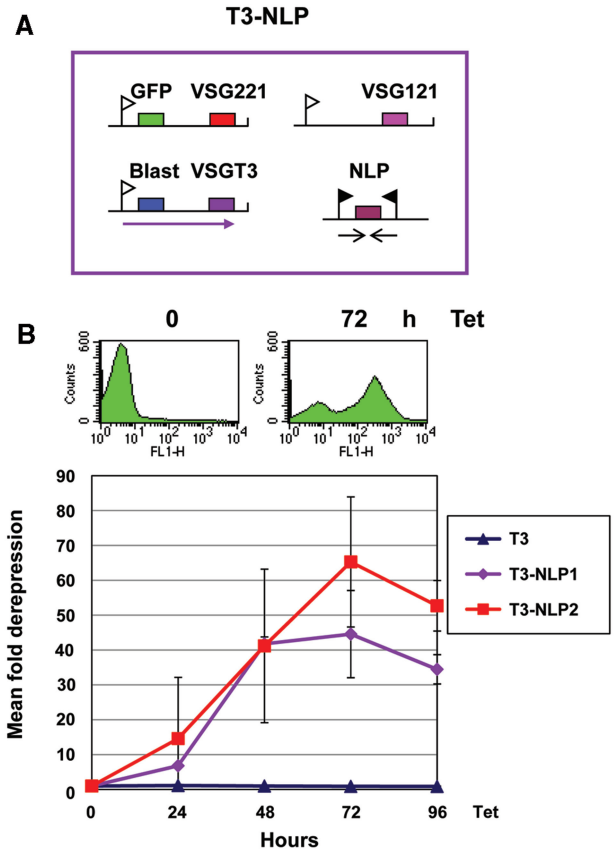

Figure 3. Blocking synthesis of NLP in bloodstream form *T. brucei* results in derepression of the silent *VSG221* ES. (**A**) Schematic of the *T. brucei* T3-NLP line. The large box indicates a trypanosome which expresses VSGT3 from the active *VSGT3* ES (transcription indicated with an arrow). A blasticidin resistance gene has been inserted immediately downstream of the active *VSGVT3* ES promoter (indicated with a white flag), allowing maintenance of a population homogeneous for VSGT3 expression through selection on blasticidin. The silent *VSG221* ES has *eGFP* inserted immediately behind the promoter. ES derepression can be monitored after the induction of *NLP* RNAi from tetracycline inducible T7 promoters (black flags). (**B**) The silent *VSG221* ES is 45–65-fold derepressed after the induction of *NLP* RNAi with tetracycline (Tet) for the time indicated in hours (h). *T. brucei* T3-NLP1 and *T. brucei* T3-NLP2 are compared with the parental *T. brucei* VSGT3 expressor (T3). Above are representative flow-cytometry traces in the FL1 channel after the induction of *NLP* RNAi for 0 or 72 h. Below is a graph showing the fold derepression at each time point calculated by dividing the mean fluorescence of a tetracycline induced culture with an uninduced culture at the same time point. Error bars show the standard deviation between three experiments.

Figure 4A). The blasticidin resistance gene used for selection in this construct is driven by an rDNA promoter. Induction of *NLP* RNAi resulted in 5–6-fold derepression of *eGFP*, indicating that NLP plays a role in silencing the minichromosomal 177-bp repeat regions. Although the degree of derepression is ~10-fold higher in the *T. brucei* T3-SM line compared with the MCEP line, the FL1-H signal after 72 h induction of *NLP* RNAi is comparable. This is explained by the low basal level of transcription from the ES promoter inserted into a transcriptionally silent minichromosome (as seen in the FACS trace for time point 0 in Figure 4A). An equivalent *T. brucei* reporter line which contained a construct without an ES promoter upstream of *eGFP* inserted into minichromosomes was also tested. Induction of *NLP* RNAi in this second cell line did not result in a significant increase in *eGFP* transcription (data not shown). This indicates that although blocking the synthesis of NLP appears to facilitate transcription from the ES promoter, it does not lead to a significant increase in fortuitous initiation of transcription from cryptic promoters at minichromosomes.

As it had earlier been shown that the ES promoter is particularly repressed if integrated into the *VSG* Basic Copy arrays of bloodstream form *T. brucei* (36), we next investigated the role of NLP in silencing this area of the genome. The VBEP construct, containing an ES promoter upstream of *eGFP*, was integrated upstream of the silent *VSG118* Basic Copy gene (Figure 4B). As seen after integrating an exogenous ES promoter in the minichromosomes, there is a low rate of transcription from an ES promoter integrated into the *VSG* Basic Copy arrays. Blocking synthesis of NLP led to a ~5-fold derepression of *eGFP* by 72 h (Figure 4B). As in the minichromosome targeting experiments, a comparable reporter line containing a construct without an ES promoter upstream of *eGFP* inserted upstream of the *VSG118* Basic Copy gene did not show significantly increased transcription of *eGFP* after the induction of *NLP* RNAi (result not shown). Therefore, although NLP appears to play a role in establishing the repressive chromatin environment silencing the exogenous ES promoter in the *VSG* Basic Copy arrays, depleting its synthesis does not result in a significant increase in fortuitous initiation of transcription from cryptic promoters in this genomic region. Our observed derepression of *eGFP* is not simply the consequence of a lethal phenotype, as induction of RNAi against the essential TDP protein in the *T. brucei* MCEP and VBEP cell lines did not lead to an increase in *eGFP* transcription (27) (results not shown).

Lastly, the role of NLP was investigated in silencing procyclin genes, which are to a great extent transcriptionally inactive in bloodstream form *T. brucei* (39,40). We used a cell line where a reporter construct was integrated behind the silent EP1 promoter in bloodstream form *T. brucei*. Although procyclin protein is not detectably expressed in bloodstream form *T. brucei,* there is a small amount of transcription from procyclin promoters. This explains the observed *eGFP* fluorescence in the FACS trace at time point 0 in Figure 4C. Blocking synthesis of NLP leads to a ~4-fold increase in transcription of *eGFP* driven by the silenced EP1 promoter (Figure 4C). In summary, blocking the synthesis of NLP had the most spectacular effect on derepressing silent *VSG* ESs in bloodstream form *T. brucei*. However, it also appears to play a role in establishing a repressive transcriptional environment for the ES promoter in bloodstream form *T. brucei* at different genomic regions, including the transcriptionally silent *T. brucei* minichromosomes, the *VSG* Basic Copy arrays and the inactive *EP1* transcription units.

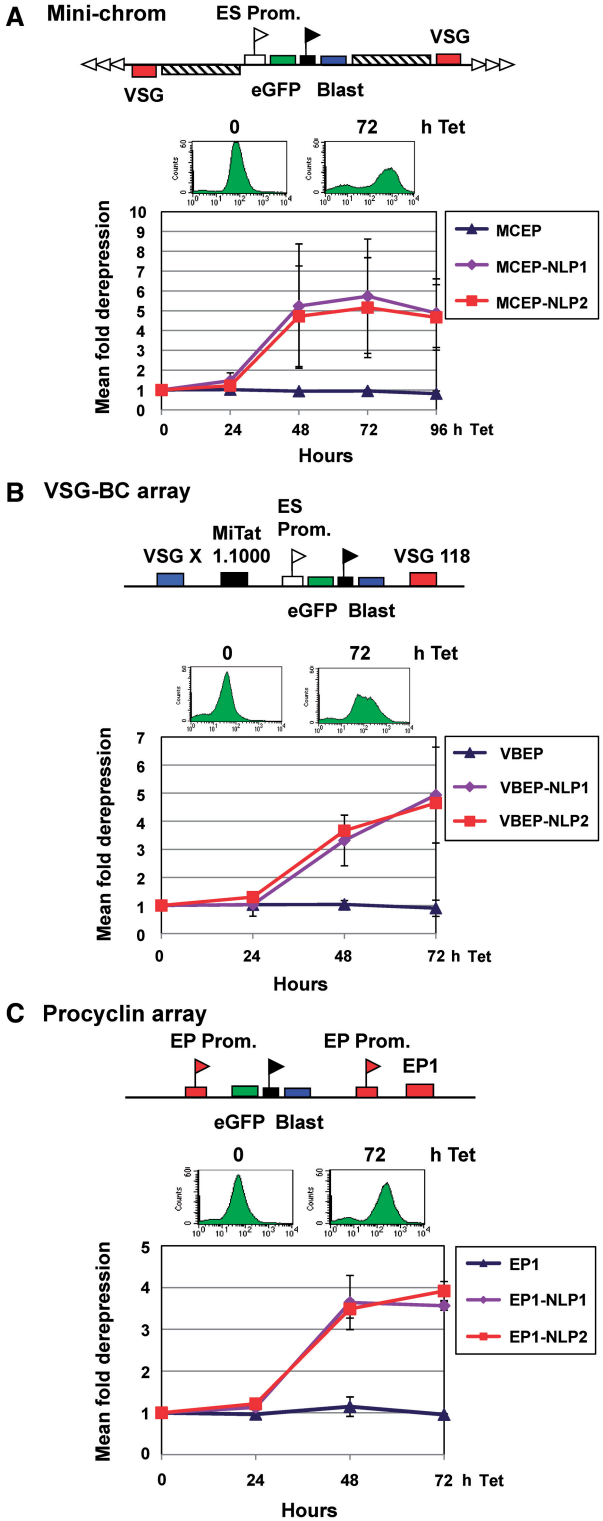

Figure 4. NLP plays a role in silencing transcriptionally inactive regions of the bloodstream form *T. brucei* genome. (**A**) Blocking synthesis of NLP leads to derepression of an ES promoter located in a transcriptionally silent minichromosome (Mini-chrom). A construct containing an ES promoter (white flag) was inserted into a *T. brucei* minichromosome using characteristic 177-bp repeat sequences which make up the bulk of the minichromosomes (diagonally hatched box). Silent *VSG*s are located at the telomeres, which are indicated with horizontal triangles. The blasticidin resistance gene (Blast) used for selection is driven by an rDNA promoter (black flag). The *T. brucei* MCEP-NLP1 and MCEP-NLP2 lines were monitored for derepression of the ES promoter using flow cytometry after the induction of *NLP* RNAi with tetracycline (Tet) for the time indicated in hours (h). Analysis of the parental *T. brucei* MCEP line is shown for comparison. Characteristic FACS traces are shown above. The results are the mean of triplicate *NLP* RNAi experiments with the standard deviation indicated with error bars. (**B**) Blocking synthesis of NLP leads to derepression of an ES promoter inserted into a transcriptionally silent *VSG* Basic Copy (BC) array. The experiment was performed as in (A) where a similar construct containing an ES promoter was inserted into the *VSG118* Basic Copy array, with *VSGX, MiTat1.100* and *VSG118* indicated with coloured boxes. Derepression of *eGFP* was monitored by flow cytometry. Above are representative flow cytometry traces after the induction of *NLP* RNAi with tetracycline. The *T. brucei* VBEP-NLP1 and *T. brucei* VBEP-NLP2 cell lines are compared with the parental *T. brucei* VBEP line. (**C**) Induction of *NLP* RNAi results in derepression of an endogenous procyclin EP1 promoter in bloodstream form *T. brucei*. The EP1 promoters (including the duplicated EP1 promoter from the construct) are indicated with red flags. Similar to panels (A) and (B), derepression of *eGFP* was monitored by flow cytometry after the induction of *NLP* RNAi with tetracycline for the time indicated. The *T. brucei* EP1-NLP1 and EP1-NLP2 lines are compared with the parental *T. brucei* EP1 cell line.

Binding of NLP is enriched in certain non-transcribed regions of the *T. brucei* genome

We next attempted to determine where NLP binds in the *T. brucei* genome using ChIP experiments. For this purpose, we used bloodstream form *T. brucei* cell lines where the carboxy terminus of one NLP allele had been epitope tagged with the HA epitope (Figure 2A). We cross-linked chromatin using formaldehyde in bloodstream form *T. brucei,* and used an antibody against the HA-tag to immunoprecipitate NLP-HA cross-linked to DNA. As a positive control, we also performed the ChIP experiment with an antibody to histone H3, or as a negative control performed the ChIP procedure without using an antibody (18). The ChIP procedure was also carried out using the parental *T. brucei* 221GPI(VO2+) cells to provide an additional negative control for specificity of the anti-HA antibody.

As NLP had originally been identified binding the 177-bp repeats, we first investigated its distribution on these sequences. Slot blot analysis showed that NLP indeed binds the 177-bp repeats (Figure 5A). In addition, NLP was found binding the 50-bp repeats which extend as large arrays upstream of all known *T. brucei* ESs, at levels that were ~3- to 4-fold background, with non-overlapping error bars indicating standard deviation (Figure 5A). We also analysed the presence of NLP in various other genomic locations. Quantitative PCR (qPCR) was performed on the input chromatin, as well as immunoprecipitated material from the *T. brucei* NLP–HA and parental cell lines to detect the presence of NLP. Schematics of the different transcription units investigated are shown in Figure 5. NLP was found at the spliced leader (SL) genes transcribed by RNA polymerase II (Figure 5B and D) (41) as well as at the 5S rRNA transcription units transcribed by RNA polymerase III (Figure 5C and D). Here also, we found relatively high amounts of NLP binding both in the intergenic spacers and within the genes themselves.

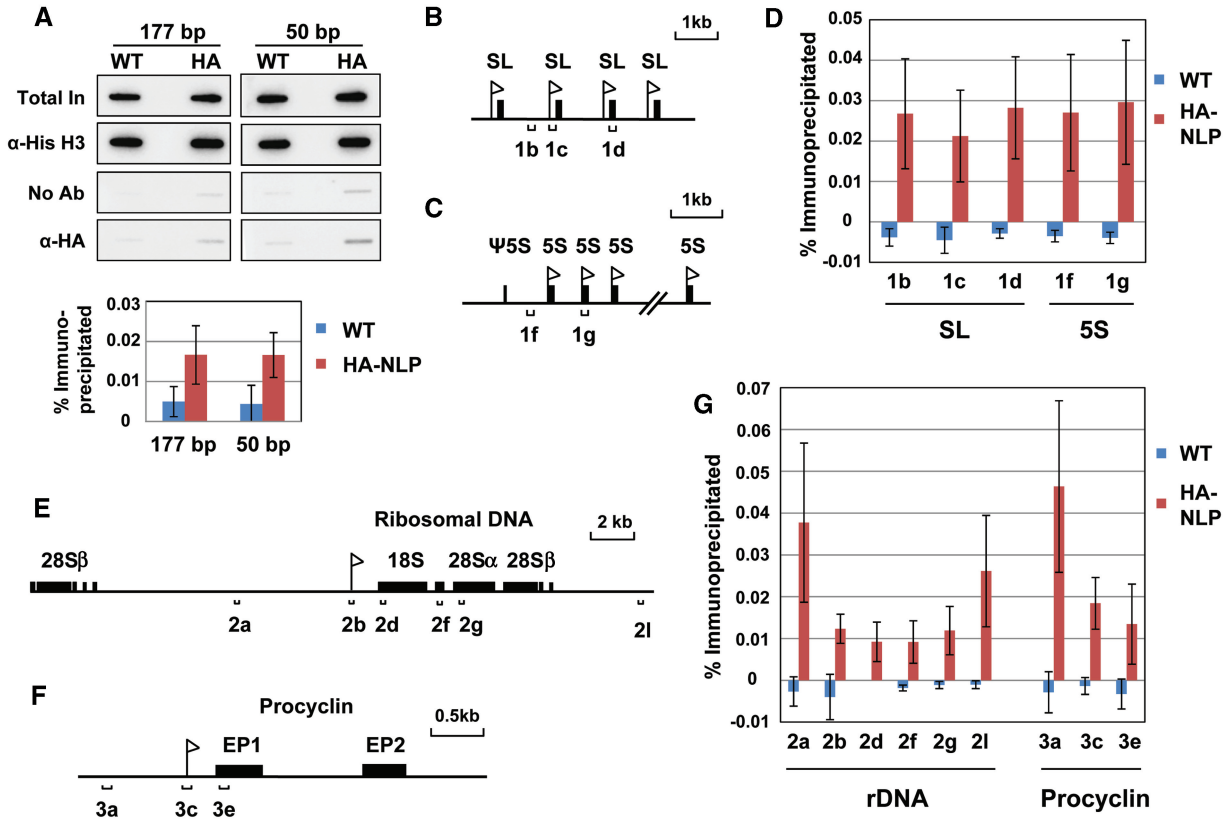

Figure 5. ChIP experiments show enrichment of NLP in simple sequence repeats as well as the non-transcribed regions around the rDNA and procyclin loci. The bloodstream form *T. brucei* HA–NLP cell line containing one allele of *NLP* tagged with the HA epitope (HA–NLP) (red bars), or the parental wild-type cell line (WT) (blue bars) was used. In all of these experiments immunoprecipitation with an anti-HA antibody was performed, and the relative amount immunoprecipitated is shown after subtraction of the values quantitated in a corresponding ChIP experiment performed in the absence of antibody. Primer pairs used for quantitative PCR (qPCR) in these ChIP experiments are indicated with numbered brackets, and are described in (18) or Supplementary Table S1. All graphs show the mean of triplicate ChIP experiments, with standard deviation indicated with error bars. (**A**) NLP is enriched on the 177-bp repeats comprising *T. brucei* minichromosomes, as well as the 50-bp repeats present upstream of all known ESs. Representative slot blots of immunoprecipitated chromatin hybridized with probes for the relevant repeat region are shown. Material from the parental cell line (WT) is compared with that from the HA–NLP line (HA). Total input (Total In) is compared with material precipitated either with an anti-histone H3 antibody (α-His H3), no antibody (No Ab) or an anti-HA epitope antibody (α-HA). A graph showing the amounts immunoprecipitated (after subtraction of the no antibody control) is indicated below the slot blot. Error bars indicate the standard deviation from three independent experiments. (**B**) Schematic diagram showing the spliced leader (SL) RNA transcription units transcribed by RNA polymerase II. The relevant genes are indicated with black boxes, with the SL promoters indicated with flags. (**C**) Diagram of the 5S rRNA locus transcribed by RNA polymerase III. The 5S genes and pseudo-gene (ψ) are indicated with black boxes and the 5S promoters with flags. (**D**) Quantitation of ChIP results using the *T. brucei* HA–NLP and parental wild-type (WT) cell lines. Immunoprecipitation with an anti-HA antibody was performed, and the relative amount of SL DNA or 5S rDNA immunoprecipitated is shown after subtraction of the values quantitated in a corresponding ChIP experiment using no antibody. (**E**) Diagram of a typical Pol I transcribed ribosomal DNA (rDNA) locus with the rDNA promoter indicated with a flag. (**F**) Schematic of the Pol I transcribed procyclin EP locus with two tandem EP genes indicated with black boxes. The EP promoter is indicated with a flag. (**G**) Quantitation of ChIP results as in D). Immunoprecipitation with an anti-HA antibody was performed, and the relative amount of rDNA or procyclin DNA immunoprecipitated is shown.

RNA polymerase I transcribes procyclin and *VSG* genes as well as the rDNA in *T. brucei* (35). First NLP distribution within the rDNA was determined. Relatively low levels of NLP were found within the rDNA transcription unit (primers 2b, 2d, 2f and 2g in Figure 5E and G). However, levels of NLP were enriched in the non-transcribed rDNA spacer either upstream or downstream of a given rDNA transcription unit (primers 2a and 2l; Figure 5E and G). Compared with levels of NLP in the 18S or 28S rDNA, levels of NLP were over 3-fold higher using primer pair 2a and nearly 3-fold using primer pair 2l. An approximately 3-fold higher level of NLP was also found upstream of the procyclin *EP1* and *EP2* transcription units (primer 3a in Figure 5F and G) compared to within the *EP1* gene itself (primer 3c and 3e). In summary, in a variety of *T. brucei* transcription units, higher levels of NLP are found binding the adjacent transcriptionally silent regions compared to within the transcription units themselves.

As downregulation of NLP leads to striking levels of derepression of silent ESs, we next investigated its binding to ES sequences (Figure 6). As ESs are highly similar to each other in sequence (12), primers can be expected to bind most if not all ESs. To circumvent this problem, we performed ChIP in a bloodstream form *T. brucei* line that contained a single copy neomycin

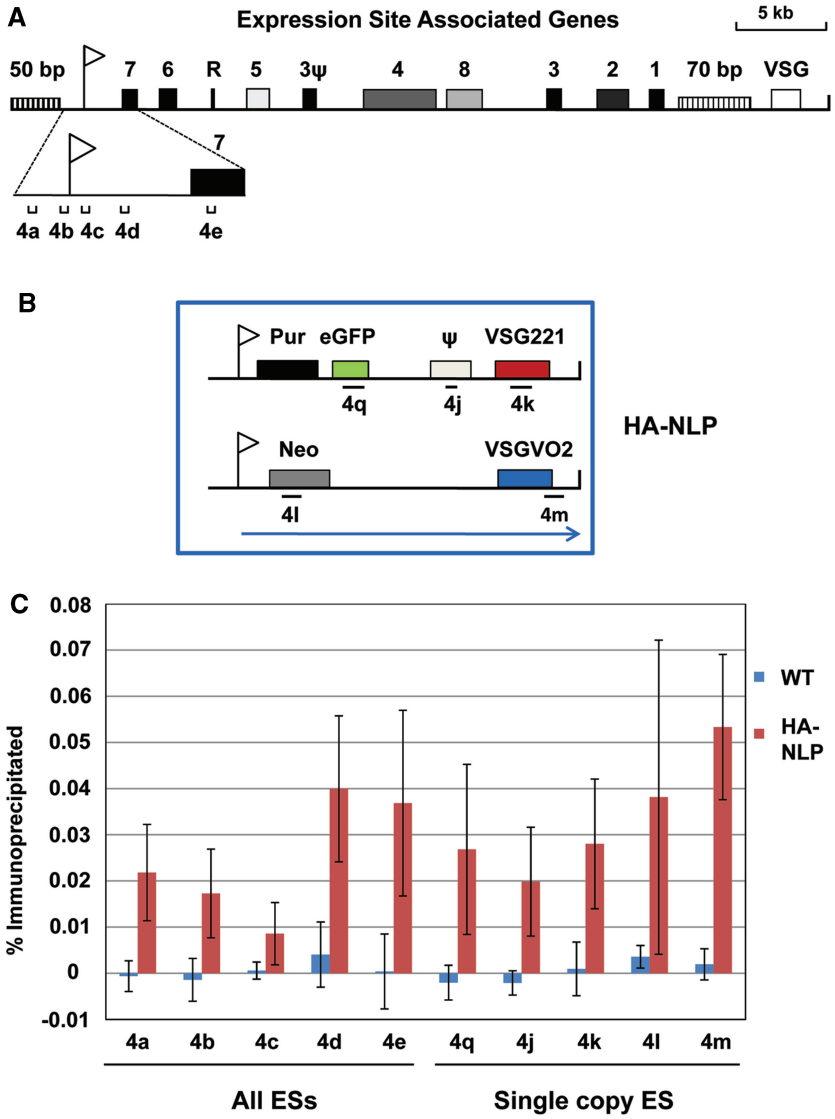

Figure 6. NLP is relatively depleted at ES promoters but binds both active and silent ESs. ChIP experiments were performed with the *T. brucei* HA–NLP and parental wild-type (WT) cell lines. (**A**) A schematic of a typical ES is shown above with the ES promoter shown with a flag, and characteristic Expression site associated genes (*ESAG*s) indicated with filled boxes. The immediate area around the ES promoter is expanded below. Characteristic 50-bp repeat arrays flanking the ES promoter, or 70-bp repeat sequences present upstream of the telomeric *VSG* are indicated with vertically striped boxes. Primers used are as described in (18). As ESs are multi-copy and highly similar, these primers can be expected to recognise most if not all ESs. (**B**) Schematic of the *T. brucei* HA–NLP cell line used for ChIP. Transcription of the active *VSGVO2* ES from the ES promoter (flag) is indicated with an arrow. The single copy neomycin resistance gene is indicated (Neo). The silent *VSG221* ES contains a construct containing a puromycin resistance gene (Pur) and *eGFP*. Other single copy genes are the single copy *VSG* pseudogene (ψ), as well as *VSG221*. These single copy genes are indicated with filled boxes. Relevant primers are indicated with numbered brackets. Primers used are as described in (18) or in Supplementary Table S1. (**C**) Quantification of the immunoprecipitated material using an anti-HA antibody to detect the HA-epitope tagged NLP using either the *T. brucei* HA–NLP cell line (HA–NLP) (red bars) or the wild-type cell line (WT) (blue bars) after subtraction of the no antibody control as described in Figure 5. Results are the mean of triplicate ChIP experiments, with standard deviation indicated with error bars.

resistance gene immediately downstream of the promoter of the active VSGVO2 ES, as well as a construct containing a puromycin resistance gene and *eGFP* behind the silent *VSG221* ES promoter (Figure 6B). The *VSG* pseudogene (ψ) and the *VSG221* gene are additional single copy sequences present within the silent *VSG221* ES. All of the common ES primers used ('All ESs' in Figure 6C) can be expected to recognise the active as well as most if not all of the silent ESs. Although we were able to find a low amount of NLP binding within the ES promoter region (primer 4c in Figure 6C), we could not distinguish between active and silent ESs with this primer set. qPCR analysis using single copy sequences specific for either the active or silent ES showed NLP binding to both silent and active ESs along the length of the telomere.

The levels of NLP immunoprecipitated in our experiments are low, but comparable to those observed for some chromatin remodeling proteins in other systems, for example ISWI in *Drosophila* (42,43). Typically, in our

experiments HA–NLP immunoprecipitation was ten to 30-fold enriched over background levels obtained after immunoprecipitation with an anti-HA antibody in wild-type cell line. The relative inefficiency of NLP ChIP compared with the histone H3 ChIP control (results not shown) (18), is presumably due to the relatively low affinity of NLP for DNA, as one might expect for a nucleoplasmin-like protein compared with a histone or a specific transcription factor.

Depletion of NLP leads to reduced transcription of the active ES

As induction of *NLP* RNAi resulted in 45- to 65-fold derepression of an *eGFP* gene present immediately downstream of the inactive *VSG221* ES promoter, we next wanted to know if this derepression led to fully processive ES transcription resulting in full activation of silent ESs or increased *VSG* ES switching. Total RNA was isolated from bloodstream form *T. brucei* NLP1 after the induction of *NLP* RNAi for different time points, cDNA was prepared and levels of various transcripts were monitored by qPCR. As expected, induction of *NLP* RNAi led to a reduction in *NLP* transcript down to ~25% normal levels by 48 h (Figure 7). Also as expected from the flow cytometry data which showed an increase in eGFP protein (Figure 3), *eGFP* transcript from the derepressed *VSG221* promoter increased almost 20-fold after the induction of *NLP* RNAi. However, despite the striking derepression of the *VSG221* ES promoter observed after the induction of *NLP* RNAi, there was no significant increase in the *VSG* transcripts themselves from a selection of six silent *VSG* ESs. *VSG* transcripts monitored include those from the *VSG13, VSG121, VSG224, VSG800, VSGbR2* and *VSGJS1* ESs (12,44). *VSG* transcripts from silent ESs were particularly low after the induction of *NLP* RNAi for 48 h. The subsequent increase in these transcripts at 72 h could be a consequence of increases in levels of NLP, possibly as a result of the emergence of revertants escaping a lethal RNAi phenotype.

A striking observation from these experiments is that the level of the active *VSGT3* transcript itself fell drastically to 4% normal levels after 48 h induction of *NLP* RNAi. Levels of transcript from the blasticidin resistance gene present in the active *VSGT3* ES also fell almost

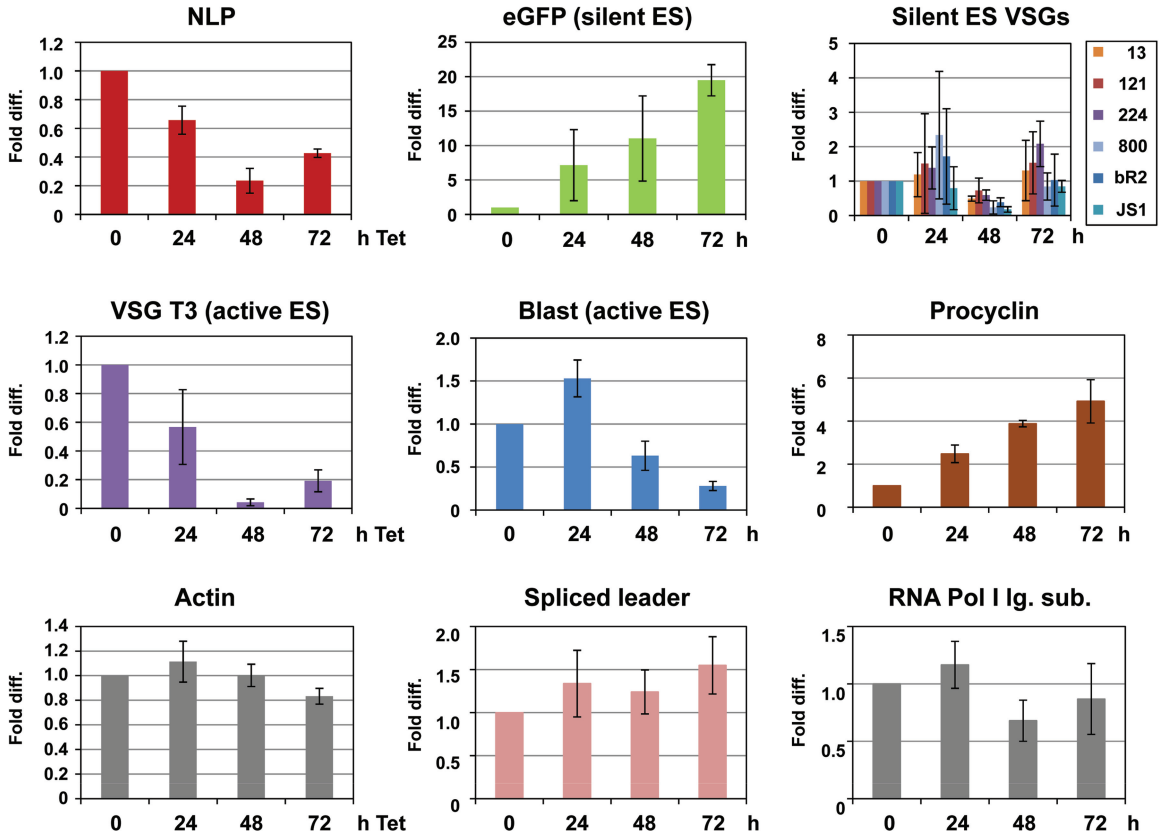

Figure 7. Quantitation of transcripts in the *T. brucei* T3-NLP1 cell line after the induction of *NLP* RNAi with tetracycline (Tet) for the time indicated in hours (h). RNA was collected from cells at different time points, cDNA was prepared and qPCR was performed to monitor changes in transcript levels. Data was normalized to the level of actin transcript at each time point, and is plotted as the fold difference between the induced and uninduced time points. Relative levels of transcript after the induction of *NLP* RNAi are shown for: *NLP*, *eGFP* present in the silent *VSG221* ES, a representative number of silent ES-located *VSGs*, *VSGT3* and the blastidin resistance gene (Blast) present in the active *VSGT3* ES, EP1 procyclin, spliced leader and the genes encoding actin and the large subunit of RNA polymerase I. The silent *VSG*s are all located at the telomeres of silent ESs, and are: *VSG13*, *VSG121*, *VSG224*, *VSG800*, *VSGbR2* and *VSGJS1* (12,44). All data shown are the mean of triplicate RNAi induction experiments with standard deviation represented with error bars. The data was normalized against the values for actin transcript shown in this figure, with the exception of the quantitation of the EP1 procyclin transcript, which was part of a separate triplicate experiment and normalized to an independent quantitation of actin.

3-fold after the induction of *NLP* RNAi for 72 h. These results indicate that NLP plays an important role in facilitating fully processive transcription from the active *VSG* ES as well as silencing the silent ESs. This lack of processive transcription from the active ES in the face of an NLP synthesis block could explain why transcripts from silent *VSG* ESs also appear reduced after 48 h. Levels of *VSG* transcripts from the active and silent *VSG*s were comparable irrespective of whether the cells had been maintained on blasticidin selection to select for continued expression of VSGT3. These results were also confirmed using an analogous bloodstream form *T. brucei* cell line expressing *VSG121* rather than *VSGT3* from the active ES, even though the degree of NLP knockdown was less pronounced in this cell line (Supplementary Figure S4).

Transcripts derived from the Pol I transcribed EP1 procyclin genes increased ~5-fold after the induction of a block in NLP synthesis (Figure 7), in agreement with the observed derepression of the EP1 procyclin promoter (see Figure 4C). In these experiments performed in triplicate, transcript amounts are presented as normalized to the amount of actin transcript present at each time point. As a reference point, the amount of actin transcript quantitated at each time point after the induction of *NLP* RNAi is also shown (Figure 7). Quantitated levels of the spliced leader or the transcripts encoding actin or the RNA polymerase I large subunit did not change significantly after NLP knockdown (Figure 7).

DISCUSSION

Here we describe a novel transcription regulatory protein NLP, which is essential, and has a nucleoplasmin-like domain and an AT-hook motif. *T. brucei* NLP plays a key role in ES control, as blocking its synthesis leads to 45- to 65-fold derepression of silent ESs. NLP also plays a role in silencing other transcriptionally inactive areas in bloodstream form *T. brucei* including the minichromosomes, the *VSG* Basic Copy arrays and the procyclin locus. Using ChIP analysis, NLP was found to bind simple sequence repeats as well as certain silent areas around Pol I transcription units in the *T. brucei* genome. However, despite the observed derepression of silent ESs after the induction of *NLP* RNAi, we did not find evidence that NLP preferentially binds silent ESs. Also, in spite of the striking degree of derepression of ES promoters observed after NLP knockdown, we did not find fully processive transcription of silent ESs or an observable increase in ES switching. Blocking synthesis of NLP resulted in a drastic reduction in processive transcription of the active ES. As one needs to have full activation of silent ESs in order to see an increase in *VSG* ES switching, the observed lack of change in *VSG* switching could be a consequence of the lack of processive transcription in the derepressed silent (as well as active) *VSG* ESs.

It has only recently become apparent that ES regulation in bloodstream form *T. brucei* involves chromatin remodeling. It is now clear that the active ES in bloodstream form *T. brucei* is radically depleted in nucleosomes compared with the silent ESs (17,18). Therefore chromatin remodeling is highly likely to be involved in the conversion of an ES from its silent to active state. The first chromatin remodeler identified to be involved in ES silencing in *T. brucei* was TbISWI, which is a member of the SNF2 superfamily of ATP-dependent chromatin remodeling complexes (19). Knockdown of TbISWI results in 30–60-fold derepression of silent ESs. In addition, the telomere binding protein TbRAP1 is involved in a gradient of silencing operating at and increasing in strength towards the ES chromosome end (20). Blocking synthesis of TbRAP1 results in an increase in ES switching as well as ES promoter derepression. Lastly, the histone methyltransferase DOT1B appears to be essential for mono-allelic expression of VSG (21). Inhibition of DOT1B synthesis results in silent ESs becoming partially derepressed, with the full switch from one ES to another occurring at a slower rate than average.

NLP does not closely resemble known chromatin remodeling proteins in other eukaryotes, and is a new addition to the small list of proteins shown to be involved in ES control in *T. brucei*. One of its distinctive features is a nucleoplasmin motif, which is similar in size to a typical nucleoplasmin protein. Nucleoplasmins are small (~150–300 amino acids) acidic proteins which function as histone chaperones (45,46). Nucleoplasmin was originally identified in *Xenopus* oocytes as a highly abundant protein which can assemble nucleosome cores *in vitro* from purified histones and DNA (31). Nucleoplasmin mediates sperm chromatin decondensation in *Xenopus* where it binds and removes sperm basic proteins and replaces them with histones H2A and H2B (47,48). In addition, nucleoplasmin has been shown to be important for regulating the chromatin condensation that occurs during apoptosis (49). In *Drosophila* a nucleoplasmin like protein (dNLP) binds to core histones, and functions in assembling regularly spaced nucleosomal arrays in an ATP-dependent fashion (50).

Is NLP a nucleoplasmin? Nucleoplasmins are typically small phosphoproteins which can function as pentamers (51). NLP at almost 1000 amino acids is more than five times bigger than a typical nucleoplasmin. In addition, it contains a non-typical AT-hook domain. AT-hook motifs are small (~11 amino acid) DNA binding motifs centred around a GRP tripeptide, which is necessary and sufficient to mediate DNA binding (33). This motif typically functions as an auxiliary protein motif, which in conjunction with other DNA binding motifs in the same protein facilitates binding to DNA (34). The AT-hook motif has also been found in a very wide variety of different DNA binding proteins including transcription regulators and co-factors of different DNA binding proteins (34). *T. brucei* NLP does not appear to be a nucleoplasmin in the strict sense of the word, but the homology to this type of protein could indicate that it interacts with histones in trypanosomes. Further experiments will be required to address this issue.

What is the role of NLP in the mono-allelic exclusion of ESs in bloodstream *T. brucei*? NLP was originally identified in DNA affinity chromatography experiments using procyclic form *T. brucei* extracts, and is not

specific to bloodstream form trypanosomes. Compatible with being a general transcription regulator, levels of NLP protein appear to be equivalent in both procyclic and bloodstream form *T. brucei* life-cycle stages. In bloodstream form trypanosomes, in addition to its importance for the establishment of ES silencing, NLP also plays a role in silencing other transcriptionally inactive regions including the minichromosomes, *VSG* Basic Copy arrays and the procyclin loci. This indicates that NLP is a general transcription regulator, and is not uniquely involved in ES control. This is consistent with its localisation in ChIP experiments to the rDNA non-transcribed spacer, and the region upstream of the Pol I transcribed procyclin loci. In the ES itself, NLP appears to bind both silent and active ESs indicating that it could play a functional role in both locations.

Compatible with this observation, knockdown of NLP synthesis resulted in reduced transcription from the active Pol I transcribed ES itself. This phenomenon was not observed with the Pol II transcribed actin, tubulin or RNA polymerase I large subunit transcripts. It is possible that chromatin remodeling is required to maintain transcription of the regulated ESs, which are transcribed in trypanosomes at a very high rate. In contrast, there does not appear to be significant transcriptional regulation of the Pol II transcribed arrays of housekeeping genes. NLP could have chromatin remodeling activity which is important for maintaining fully processive transcription of the active ES. This could, for example, operate through facilitating removal of histones including histone H3, which has been shown to be particularly depleted from the active ES (17,18). These different activities of NLP argue that it plays a role in both facilitating and inhibiting transcription. There is precedent for this, as the ISWI complexes in other eukaryotes provide a good example of a chromatin factor involved in both transcription repression and activation within a single cell. In *Saccharomyces cerevisiae* the Isw1a complex (consisting of Isw1p and Ioc3p) is involved in transcription silencing, while the Isw1b complex (consisting of Isw1p together with Ioc2p and Ioc4p) is involved in transcription elongation (52).

A challenge will come in determining how NLP interacts with other chromatin remodeling proteins and histone modification enzymes including ISWI, RAP1 and DOT1B in maintaining ES control. It is likely that multiple silencing gradients operate simultaneously on silent ESs in *T. brucei* (20,53). A relatively short distance repressive gradient extends up from the *T. brucei* ES telomere, and involves the sirtuin protein SIR2 (54,55). SIR2 is involved in repression operating in the immediate proximity of the telomere repeats, but does not appear to play a role in the long distance repressive effect operating over many tens of kilobases, necessary for control of the ES promoter (55). In contrast, the telomere binding protein RAP1 establishes a silencing gradient operating over much longer distances including the ES promoter, and increasing in intensity closer to the ES telomere (20). Blocking RAP1 synthesis results in derepression of silent ESs, and an increase in transcripts from *VSG*s located at silent ES telomeres.

Blocking NLP synthesis results in derepression of a silent ES promoter but no observable increase in VSG switching. One possibility is that NLP is involved in establishing or maintaining repressed chromatin in the immediate vicinity of the ES promoter. Blocking NLP synthesis could possibly result in promoter derepression, but as the derepressed chromatin is relatively localized, the Pol I does not transcribe in a processive fashion down to the telomere end. This could be the consequence of a second repressive gradient (possibly mediated by RAP1) impeding the elongating RNA polymerases. A complication with interpreting our findings however is the fact that transcription of the active ES itself is impeded by NLP knockdown. This implies that NLP could be involved in establishing the chromatin environment necessary for the elongating Pol I transcription complex. A challenge for the future will be in unravelling the interplay of the multiple regulatory factors implicated in ES control.

SUPPLEMENTARY DATA

Supplementary Data are available at NAR Online.

ACKNOWLEDGEMENTS

The authors thank Tomoko Isobe, Matthew Wand and Andrew Voak for making DNA constructs and performing initial experiments. They are very grateful to Prof. Jane Mellor (Department of Biochemistry, University of Oxford) for help with the ChIP experiments and allowing use of the BioRuptor sonicator. They are grateful to Prof. Thomas Seebeck (University of Bern) for providing epitope tagging constructs. They thank Prof. Jay Bangs (University of Wisconsin) for providing anti-BiP antibody. They are grateful to Megan Lindsay Povelones, Viola Denninger, Nadina Vasileva Wand, Simone Wiesler, Robin Chisman, Marcin Dembek and Siobhan Durran for comments on the article.

FUNDING

Wellcome Trust; G.R. is a Wellcome Senior Fellow in the Basic Biomedical Sciences; Clarendon Fund and the Queen's College Graduate Scholarship, Oxford funding to M.S.N.; Inlaks Foundation and the Clarendon Fund funding to M.K. Funding for open access charge: The Wellcome Trust.

Conflict of interest statement. None declared.

REFERENCES

1. Serizawa,S., Miyamichi,K. and Sakano,H. (2004) One neuron-one receptor rule in the mouse olfactory system. *Trends Genet*., **20**, 648–653.
2. Lomvardas,S., Barnea,G., Pisapia,D.J., Mendelsohn,M., Kirkland,J. and Axel,R. (2006) Interchromosomal interactions and olfactory receptor choice. *Cell*, **126**, 403–413.
3. Fuss,S.H., Omura,M. and Mombaerts,P. (2007) Local and cis effects of the H element on expression of odorant receptor genes in mouse. *Cell*, **130**, 373–384.

4. Scherf,A., Lopez-Rubio,J.J. and Riviere,L. (2008) Antigenic variation in Plasmodium falciparum. *Ann. Rev. Microbiol.*, **62**, 445–470.
5. Voss,T.S., Healer,J., Marty,A.J., Duffy,M.F., Thompson,J.K., Beeson,J.G., Reeder,J.C., Crabb,B.S. and Cowman,A.F. (2006) A var gene promoter controls allelic exclusion of virulence genes in Plasmodium falciparum malaria. *Nature*, **439**, 1004–1008.
6. Voss,T.S., Tonkin,C.J., Marty,A.J., Thompson,J.K., Healer,J., Crabb,B.S. and Cowman,A.F. (2007) Alterations in local chromatin environment are involved in silencing and activation of subtelomeric var genes in Plasmodium falciparum. *Mol. Microbiol.*, **66**, 139–150.
7. Frank,M. and Deitsch,K. (2006) Activation, silencing and mutually exclusive expression within the var gene family of Plasmodium falciparum. *Int. J. Parasitol.*, **36**, 975–985.
8. Horn,D. and Barry,J.D. (2005) The central roles of telomeres and subtelomeres in antigenic variation in African trypanosomes. *Chromosome Res.*, **13**, 525–533.
9. Taylor,J.E. and Rudenko,G. (2006) Switching trypanosome coats: what's in the wardrobe? *Trends Genet.*, **22**, 614–620.
10. Morrison,L.J., Marcello,L. and McCulloch,R. (2009) Antigenic variation in the African trypanosome: molecular mechanisms and phenotypic complexity. *Cell Microbiol.*, **11**, 1724–1734.
11. Berriman,M., Hall,N., Sheader,K., Bringaud,F., Tiwari,B., Isobe,T., Bowman,S., Corton,C., Clark,L., Cross,G.A. *et al.* (2002) The architecture of variant surface glycoprotein gene expression sites in Trypanosoma brucei. *Mol. Biochem. Parasitol.*, **122**, 131–140.
12. Hertz-Fowler,C., Figueiredo,L.M., Quail,M.A., Becker,M., Jackson,A., Bason,N., Brooks,K., Churcher,C., Fahkro,S., Goodhead,I. *et al.* (2008) Telomeric expression sites are highly conserved in Trypanosoma brucei. *PLoS One*, **3**, e3527.
13. Chaves,I., Rudenko,G., Dirks-Mulder,A., Cross,M. and Borst,P. (1999) Control of variant surface glycoprotein gene-expression sites in Trypanosoma brucei. *EMBO J.*, **18**, 4846–4855.
14. Rudenko,G., Blundell,P.A., Taylor,M.C., Kieft,R. and Borst,P. (1994) VSG gene expression site control in insect form Trypanosoma brucei. *EMBO J.*, **13**, 5470–5482.
15. Vanhamme,L., Poelvoorde,P., Pays,A., Tebabi,P., Van Xong,H. and Pays,E. (2000) Differential RNA elongation controls the variant surface glycoprotein gene expression sites of Trypanosoma brucei. *Mol. Microbiol.*, **36**, 328–340.
16. Navarro,M., Cross,G.A. and Wirtz,E. (1999) Trypanosoma brucei variant surface glycoprotein regulation involves coupled activation/inactivation and chromatin remodeling of expression sites. *EMBO J.*, **18**, 2265–2272.
17. Figueiredo,L.M. and Cross,G.A. (2010) Nucleosomes are depleted at the VSG expression site transcribed by RNA polymerase I in African trypanosomes. *Eukaryot. Cell*, **9**, 148–154.
18. Stanne,T.M. and Rudenko,G. (2010) Active VSG expression sites in Trypanosoma brucei are depleted of nucleosomes. *Eukaryot. Cell*, **9**, 136–147.
19. Hughes,K., Wand,M., Foulston,L., Young,R., Harley,K., Terry,S., Ersfeld,K. and Rudenko,G. (2007) A novel ISWI is involved in VSG expression site downregulation in African trypanosomes. *EMBO J.*, **26**, 2400–2410.
20. Yang,X., Figueiredo,L.M., Espinal,A., Okubo,E. and Li,B. (2009) RAP1 is essential for silencing telomeric variant surface glycoprotein genes in Trypanosoma brucei. *Cell*, **137**, 99–109.
21. Figueiredo,L.M., Janzen,C.J. and Cross,G.A. (2008) A histone methyltransferase modulates antigenic variation in African trypanosomes. *PLoS Biol.*, **6**, e161.
22. Hirumi,H. and Hirumi,K. (1989) Continuous cultivation of Trypanosoma brucei blood stream forms in a medium containing a low concentration of serum protein without feeder cell layers. *J. Parasitol.*, **75**, 985–989.
23. Wirtz,E., Leal,S., Ochatt,C. and Cross,G.A. (1999) A tightly regulated inducible expression system for conditional gene knock-outs and dominant-negative genetics in Trypanosoma brucei. *Mol. Biochem. Parasitol.*, **99**, 89–101.
24. Sheader,K., te Vruchte,D. and Rudenko,G. (2004) Bloodstream form-specific up-regulation of silent vsg expression sites and procyclin in Trypanosoma brucei after inhibition of DNA synthesis or DNA damage. *J. Biol. Chem.*, **279**, 13363–13374.
25. Oberholzer,M., Morand,S., Kunz,S. and Seebeck,T. (2006) A vector series for rapid PCR-mediated C-terminal in situ tagging of Trypanosoma brucei genes. *Mol. Biochem. Parasitol.*, **145**, 117–120.
26. Larkin,M.A., Blackshields,G., Brown,N.P., Chenna,R., McGettigan,P.A., McWilliam,H., Valentin,F., Wallace,I.M., Wilm,A., Lopez,R. *et al.* (2007) Clustal W and Clustal X version 2.0. *Bioinformatics*, **23**, 2947–2948.
27. Erondu,N.E. and Donelson,J.E. (1992) Differential expression of two mRNAs from a single gene encoding an HMG1-like DNA binding protein of African trypanosomes. *Mol. Biochem. Parasitol.*, **51**, 111–118.
28. Wickstead,B., Ersfeld,K. and Gull,K. (2002) Targeting of a tetracycline-inducible expression system to the transcriptionally silent minichromosomes of Trypanosoma brucei. *Mol. Biochem. Parasitol.*, **125**, 211–216.
29. Ligtenberg,M.J., Bitter,W., Kieft,R., Steverding,D., Janssen,H., Calafat,J. and Borst,P. (1994) Reconstitution of a surface transferrin binding complex in insect form Trypanosoma brucei. *EMBO J.*, **13**, 2565–2573.
30. Sambrook,J. and Russell,D.W. (2001) *Molecular Cloning: A Laboratory Manual*, 3rd edn. Cold Spring Harbour Press, New York, USA.
31. Earnshaw,W.C., Honda,B.M., Laskey,R.A. and Thomas,J.O. (1980) Assembly of nucleosomes: the reaction involving X. laevis nucleoplasmin. *Cell*, **21**, 373–383.
32. Eirin-Lopez,J.M., Frehlick,L.J. and Ausio,J. (2006) Long-term evolution and functional diversification in the members of the nucleophosmin/nucleoplasmin family of nuclear chaperones. *Genetics*, **173**, 1835–1850.
33. Reeves,R. and Nissen,M.S. (1990) The A.T-DNA-binding domain of mammalian high mobility group I chromosomal proteins. A novel peptide motif for recognizing DNA structure. *J. Biol. Chem.*, **265**, 8573–8582.
34. Aravind,L. and Landsman,D. (1998) AT-hook motifs identified in a wide variety of DNA-binding proteins. *Nucleic Acids Res.*, **26**, 4413–4421.
35. Gunzl,A., Bruderer,T., Laufer,G., Schimanski,B., Tu,L.C., Chung,H.M., Lee,P.T. and Lee,M.G. (2003) RNA polymerase I transcribes procyclin genes and variant surface glycoprotein gene expression sites in Trypanosoma brucei. *Eukaryot. Cell*, **2**, 542–551.
36. Horn,D. and Cross,G.A. (1997) Position-dependent and promoter-specific regulation of gene expression in Trypanosoma brucei. *EMBO J.*, **16**, 7422–7431.
37. Urmenyi,T.P. and Van der Ploeg,L.H. (1995) PARP promoter-mediated activation of a VSG expression site promoter in insect form Trypanosoma brucei. *Nucleic Acids Res.*, **23**, 1010–1018.
38. Wickstead,B., Ersfeld,K. and Gull,K. (2004) The small chromosomes of Trypanosoma brucei involved in antigenic variation are constructed around repetitive palindromes. *Genome Res.*, **14**, 1014–1024.
39. Rudenko,G., Bishop,D., Gottesdiener,K. and Van der Ploeg,L.H. (1989) Alpha-amanitin resistant transcription of protein coding genes in insect and bloodstream form Trypanosoma brucei. *EMBO J.*, **8**, 4259–4263.
40. Roditi,I., Furger,A., Ruepp,S., Schurch,N. and Butikofer,P. (1998) Unravelling the procyclin coat of Trypanosoma brucei. *Mol. Biochem. Parasitol.*, **91**, 117–130.
41. Aksoy,S., Williams,S., Chang,S. and Richards,F.F. (1990) SLACS retrotransposon from Trypanosoma brucei gambiense is similar to mammalian LINEs. *Nucleic Acids Res.*, **18**, 785–792.
42. Song,H., Spichiger-Haeusermann,C. and Basler,K. (2009) The ISWI-containing NURF complex regulates the output of the canonical Wingless pathway. *EMBO Rep.*, **10**, 1140–1146.
43. Liu,Y.I., Chang,M.V., Li,H.E., Barolo,S., Chang,J.L., Blauwkamp,T.A. and Cadigan,K.M. (2008) The chromatin remodelers ISWI and ACF1 directly repress Wingless transcriptional targets. *Dev. Biol.*, **323**, 41–52.
44. Aitcheson,N., Talbot,S., Shapiro,J., Hughes,K., Adkin,C., Butt,T., Sheader,K. and Rudenko,G. (2005) VSG switching in Trypanosoma brucei: antigenic variation analysed using RNAi in the absence of immune selection. *Mol. Microbiol.*, **57**, 1608–1622.

45. Eitoku,M., Sato,L., Senda,T. and Horikoshi,M. (2008) Histone chaperones: 30 years from isolation to elucidation of the mechanisms of nucleosome assembly and disassembly. *Cell. Mol. Life Sci.*, **65**, 414–444.
46. Frehlick,L.J., Eirin-Lopez,J.M. and Ausio,J. (2007) New insights into the nucleophosmin/nucleoplasmin family of nuclear chaperones. *Bioessays*, **29**, 49–59.
47. Philpott,A., Leno,G.H. and Laskey,R.A. (1991) Sperm decondensation in Xenopus egg cytoplasm is mediated by nucleoplasmin. *Cell*, **65**, 569–578.
48. Laskey,R.A., Mills,A.D., Philpott,A., Leno,G.H., Dilworth,S.M. and Dingwall,C. (1993) The role of nucleoplasmin in chromatin assembly and disassembly. *Philos. Trans. R. Soc. Lond. B Biol. Sci.*, **339**, 263–269; discussion 268–269.
49. Lu,Z., Zhang,C. and Zhai,Z. (2005) Nucleoplasmin regulates chromatin condensation during apoptosis. *Proc. Natl Acad. Sci. USA*, **102**, 2778–2783.
50. Ito,T., Tyler,J.K., Bulger,M., Kobayashi,R. and Kadonaga,J.T. (1996) ATP-facilitated chromatin assembly with a nucleoplasmin-like protein from Drosophila melanogaster. *J. Biol. Chem.*, **271**, 25041–25048.
51. Taneva,S.G., Banuelos,S., Falces,J., Arregi,I., Muga,A., Konarev,P.V., Svergun,D.I., Velazquez-Campoy,A. and Urbaneja,M.A. (2009) A mechanism for histone chaperoning activity of nucleoplasmin: thermodynamic and structural models. *J. Mol. Biol.*, **393**, 448–463.
52. Mellor,J. and Morillon,A. (2004) ISWI complexes in Saccharomyces cerevisiae. *Biochim. Biophys. Acta*, **1677**, 100–112.
53. Horn,D. (2009) Antigenic variation: extending the reach of telomeric silencing. *Curr. Biol.*, **19**, R496–498.
54. Glover,L. and Horn,D. (2006) Repression of polymerase I-mediated gene expression at Trypanosoma brucei telomeres. *EMBO Rep.*, **7**, 93–99.
55. Alsford,S., Kawahara,T., Isamah,C. and Horn,D. (2007) A sirtuin in the African trypanosome is involved in both DNA repair and telomeric gene silencing but is not required for antigenic variation. *Mol. Microbiol.*, **63**, 724–736.